Investigating nuclei produced in ^{9}Li +^{11}B reaction

Margareta Sigmund[1,*], *Neven* Soić[1], *Martin* Alcorta Moreno[2], *Jack* Bishop[3], *Alexander D.* Brooks[3], *Thomas* Davinson[4], *Daniele* Dell'Aquila[5,6], *Alessia* Di Pietro[7], *Fillippo* Falezza[3], *Martin* Freer[3], *Igor* Gašparić[1], *Deša* Jelavić Malenica[1], *Tzany* Kokalova Wheldon[3], *Marco* La Cognata[7], *Annika* Lennarz[2], *Ivana* Lihtar[1], *Ismael* Martel Bravo[8], *Matko* Milin[9], *Claus* Müller Gatermann[10], *Cody* Parker[11,**], and *Nikola* Vukman[1,12,***]

[1]Institut Ruđer Bošković, Zagreb, Croatia
[2]TRIUMF, Vancouver, BC, Canada
[3]School of Physics and Astronomy, University of Birmingham, Birmingham, UK
[4]School of Physics and Astronomy, University of Edinburgh, Edinburgh, UK
[5]Department of Physics "Ettore Pancini", Università degli Studi di Napoli "Federico II", Naples, Italy
[6]INFN - Sezione di Napoli, Naples, Italy
[7]INFN - Laboratori Nazionali del Sud, Catania, Italy
[8]Department of Applied Physics, University of Huelva, Huelva, Spain
[9]Department of Physics, Faculty of Science, University of Zagreb, Zagreb, Croatia
[10]Argonne National Laboratory, Lemont, IL, USA
[11]Texas A&M University, College Station, Texas, USA
[12]INFN - Sezione di Perugia, Perugia, Italy

Abstract. In this contribution, a preliminary analysis of the first part of the experiment S2012 conducted at the ISAC-II facility of Canada's particle accelerator center TRIUMF in Vancouver will be presented. The experiment aims to study highly clustered structures of nuclei created in multi-nucleon transfer reactions of ^{9}Li radioactive beam on natural boron target (^{11}B and ^{10}B). The main objective of the experiment is to study exotic structures created in neutron-rich ^{16}C nucleus in the range of higher excitation energies. The analysis presented here probes the existence of exotic cluster configurations and the quality of detected results using the invariant mass techniques.

1 Introduction

Clustering, or the emergence of substructures as an energetically more favorable nucleon arrangement, is an important phenomenon appearing in nuclei as a consequence of the complex nucleon-nucleon interactions [1–3]. The most common substructure is alpha particle, which makes clustering most pronounced in self-conjugated ($N = Z$) nuclei [4]. Different substructures, such as the triton [5], can also be observed apart from alpha particles. Clustering has also been observed in neutron-rich isotopes, making them one of the most attractive areas in studying light nuclei structure. In the case of neutron-rich nuclei, additional neutrons strongly affect both nuclear structure and its features. It is expected that additional neutrons are shared between "clustering centers" (i.e. alpha particle), similar to the behavior of a covalent electron inside of an atomic molecule [6]. Such nuclear structure is called a *nuclear molecule*. The influence of valence neutrons on unstable nuclei is observed already in a system with one extra neutron, for instance in the ^{9}Be nucleus. Namely, in the case of ^{9}Be, the unstable ^{8}Be nucleus becomes stable by acquiring an extra neutron.

The simplest nuclear molecules, still extensively studied, are two- and three-center ones, i.e. beryllium [7–9] and carbon [10–12] isotopes. One of the most interesting neutron-rich nuclei is ^{16}C. According to different theoretical calculations [13–15], extremely exotic structures such as linear chains are proposed to exist at higher excitation energies. Up until now, there have not been many experiments that managed to study higher excited states. So far, only the experiment performed at the Radioactive Ion Beam Line at the Heavy Ion Research Facility in Lanzhou (HIRFL-RIBLL), which used an inelastic scattering of ^{16}C beam on $(CD_2)_n$ target [16, 17], has been able to excite and measure exotic states.

The objective of the S2012 experiment performed at the ISAC-II facility [18] at TRIUMF Canada's Particle Accelerator Center was to study the ^{16}C exotic structure. For this purpose, a neutron-rich ^{9}Li radioactive beam on a ^{11}B target was used to induce multi-nucleon transfer reactions producing ^{16}C. The reaction studied in this work is highly selective in the production of excited states of several nuclear systems, such as ^{10}Be, ^{16}C, etc., due to possible multi-nucleon transfer mechanisms triggered by the

*Corresponding author: Margareta.Sigmund@irb.hr
**Present address: Department of Physics & Astronomy, Ohio University, Athens, OH USA
***Present address: Faculty of Science, University of Split, Split, Croatia

intrinsic cluster structures of projectile and target. Even though the structure of ^{9}Li has yet to be thoroughly investigated, there are some indications of its clustered structure [19, 20]. On the other hand, it is already known that ^{11}B in its excited states decays via α and triton [21], which strongly points to the clustering in its structure. Furthermore, the production reaction ^{9}Li(^{11}B, α)^{16}C*, has high Q-value: Q = 17.5037 MeV.

A preliminary analysis of the data will be discussed in this contribution. The aim is to prove the reconstruction capability of the reaction products and their initial state from emitted fragments detected in coincidence. The manuscript also discusses details of the calibration of the detection setup, which consisted of an array of silicon strip detectors, alongside preliminary results obtained using invariant mass techniques. The quality of the results confirms that the experiment successfully studies neutron-rich nuclei structures.

2 The Experiment

2.1 Beam and Targets

To populate states with highly pronounced clustered or nuclear molecular structure, a radioactive ^{9}Li beam (E = 8.31 MeV/u, intensity up to $\approx 10^{7}$ pps) with very high beam energy resolution ($\approx$ 0.5%) was used on a few different sets of natural boron targets. From the different available beams around the world, the reaction ^{11}B(^{9}Li, α)^{16}C* has the highest Q value (17.5037 MeV) to populate ^{16}C*, which increases the probability that channels of interest would be opened (higher total available energy and higher cross-section). Since the thick boron targets production is not straightforward and a large thickness (for a higher reaction rate) was needed, multiple targets with different backing and specifications were prepared for the experiment. Stacks of ^{11}B targets manufactured by the Target Fabrication Facility of the Argonne National Laboratory and by the target laboratory of National Institute for Nuclear Physics - National Laboratories of Legnaro (INFN - LNL) were used. To produce the targets, natural B (1000 μg/cm^2) was evaporated on Ta (1600 μg/cm^2) or Al (900 μg/cm^2) backings. Thinner versions of the targets were also produced, evaporating about 250 μg/cm^2 of B on a thin Al backing $\approx$ 40 μg/cm^2. Since the thinner targets are more uniform and have a higher B vs. Al ratio, two stacks of 4 combined targets were used; to have a boron target as thick as possible on a backing as thin as possible. Apart from those, multiple targets of natural boron (900 μg/cm^2) on Al, from the target laboratory of Horia Hulubei National Institute of Physics and Nuclear Engineering (IFIN - HH) from Măgurele, Romania, were delivered.

2.2 Experimental Setup

The experiment was conducted in a 1.5-m-long cylindrical (along the beam axis) TUDA (TRIUMF UK Detector Array) chamber. The huge advantage of a such-shaped chamber is that detectors can be positioned symmetrically around the beam-axis and cover a large azimuthal (ϕ) angular range for the same polar (θ) angles. In this experiment, six telescope detectors were used. Four were at the smaller θ angles (more forward angles) and two were at the larger θ angles. Each telescope detector consisted of a thick Micron Semiconductor double-sided silicon strip detector (DSSSD, 1000 μm of thickness) and a thin Micron Semiconductor single-sided silicon strip detector (SSSSD). Two telescope detectors at the more forward θ angle, up and down with respect to the beam axis, had 20 μm thick SSSSD detectors while the rest of the telescopes had 50 μm thick SSSSDs as the first stage of the detection. A photo of the setup and schematic view can be seen in Fig. 1, while the angular coverage of six telescopes can be seen in Fig. 2.

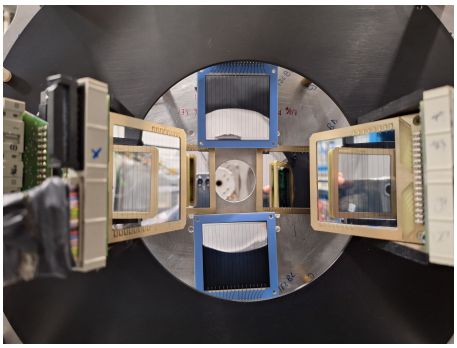

(a) Photo of an experimental setup placed around the beam axis

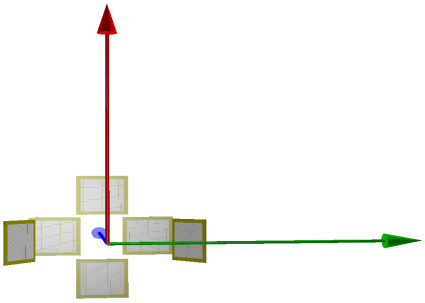

(b) Schematic of experimental setup; red line - x-axis, green line - y-axis, blue line - z-axis (beam axis)

Figure 1: Experimental setup: (a) as mounted inside the chamber and (b) schematic.

Since the reactions of interest are based on the pick-up of α + ^{3}H or stripping of $t + n + n$ reactions, we have alpha-like recoil particles going to larger θ angles or residual alpha-like particles going to forward angles, respectively. Since the main focus of the experiment was the study of the decay channels of ^{16}C* into α + ^{12}Be, ^{6}He + ^{10}Be or ^{8}He + ^{8}Be, discrimination between helium and beryllium isotopes was crucial to distinguish different ^{16}C decay channels.

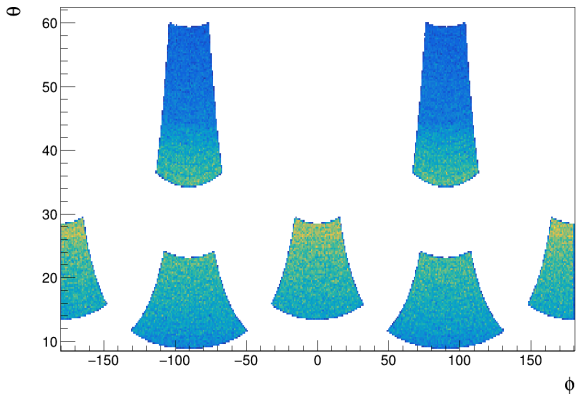

Figure 2: Angular coverage of each telescope detector in θ and ϕ angles.

2.3 Calibration

The second stage of the detection system (i.e. DSSSD detectors) is calibrated first with a combined alpha source ^{148}Gd + ^{230}Th + ^{244}Cm. The most pronounced alpha energies are at E_1 = 3182.690(24) keV, which corresponds to the alpha decay of ^{148}Gd into ^{144}Sm [22]; E_2 = 4687.0(15) keV for the alpha decay of ^{230}Th into ^{226}Ra (absolute intensity ≈ 76.3(3)%) [23] and E_3 = 5804.77(5) keV for ^{244}Cm alpha decay into ^{240}Pu (absolute intensity≈ 76.9(1)%) [24]. Once calibrated with alpha particles, each pixel (i.e. combination of front and back strip in DSSSD detector) was calibrated with elastic scattering of the stable ^{12}C beam with an energy of 5 MeV/u off the ^{11}B (1000 μg/cm^2) on Ta (1600 μg/cm^2) target. Even though both elastic scattering off ^{11}B and Ta were visible, the one from Ta was more pronounced and used for the calibration.

That completed the calibration of the second stage of detector telescopes (DSSSDs) and enabled us to start the calibration of the first stage of the detection system (SSSSDs). A 50 μm silicon detector is thick enough to stop alpha particles of all three most pronounced alpha-source energies, while the highest energy alpha-particle punches through the 20 μm SSSSDs. Therefore, 50 μm thick detectors were calibrated in the same manner as the alpha calibration of DSSSDs. Due to the varying thickness of each strip in 20 μm SSSSD, each event of alpha-particle that punched through was used as a calibration point, which allowed us to have alpha events in the range from 2600 keV up to 4000 keV. For each of those points, we had to reconstruct the corresponding energy left in the first stage from the energy left in the second stage of detection system, taking into account energy loss in "dead layers" (0.5 μm aluminum on each side of the detector). There were between 2000 and 3000 such events per strip.

2.4 Particle Identification

As mentioned above, it was crucial to have telescope detectors for particle identification. According to the Bethe-Bloch energy loss formula, once a particle goes through (or stops in) the detector, it deposits different amounts of energy according to the thickness of the detector and the kinetic energy, charge, and mass of the detected particle. When energy deposited in a SSSSD (dE on the histogram, see Fig. 3) is plotted versus the energy deposited in a DSSSD (E on the histogram), nicely separated data loci are created. It is easy to recognize which loci corresponds to ^{9}Li since it has a highly abundant pile of events around $dE \approx 6.7$ MeV and $E \approx 45$ MeV, which is populated with elastic scattering events. At the lowest dE energies, it is easy to distinguish ^{1}H, ^{2}H and ^{3}H. Above those, the most pronounced band is the one from ^{4}He, since many different reaction channels produce alpha-particles. Apart from the already mentioned particles, ^{6,8}He, ^{6,7,8,9}Li, ^{9,10}Be and ^{10,11}B are present on dE-E spectra, too. In 2001 Tassan-Got proposed [25] a new functional form for charge and mass identification that allows safe interpolation in regions with low statistics for linear response detectors, such as silicon ones. The corresponding identification loci were linearised using the extended version of the functional (for mass and charge identification), called LeNeindre enhanced functional [26] ((14 parameters), developed by the Chimera group), and suitably adapting the free parameters via standard error minimization technique. The procedure was done using DEEFIT - a program developed to simplify fitting and checking a fit's quality. An example of the function fit to data can be seen in Fig. 3b (for the sake of clarity, only one isotope of each element is fitted).

3 Preliminary results

3.1 Invariant mass method

In this experiment, only charged particles were detected. Therefore, excited states of nuclei created in the ^{9}Li and ^{11}B reactions were detectable through its decay or using the missing mass method. Here, the invariant mass method spectra of fragments detected in coincidence will be presented. It is important to mention that the time window for data acquisition was 10-μs-long, which sometimes causes overlap of different physical events in the same data acquisition period.

Invariant mass spectra were produced to prove the capability of correctly reconstructing fragments in coincidence and probing the initial state from which the fragments are emitted. The aim is to check if highly clustered states with well-known and previously measured energies were observed, and if any possible indications of interesting and rarely measured states exist. That gives us confirmation that clustered states are populated and the ability to check the energy resolution of produced coincidence spectra.

The excitation energy of a mother nucleus, assumed to decay into a group of detected fragments, can be calculated as:

$$E^* = E_{inv} - E_{g.s.}, \quad (1)$$

where E_{inv} is the invariant mass of the detected fragments and $E_{g.s.}$ is the ground-state mass of the decaying

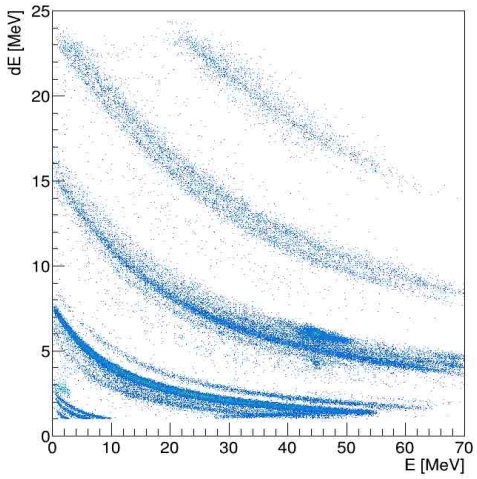

(a) An example of dE-E histogram for events in one telescope. On the figure, listed from below upwards, nicely separated data loci correspond to isotopes ^{1,2,3}H, ^{3,4,6,8}He, ^{6,7,8,9}Li, ^{9,10}Be and ^{10,11}B

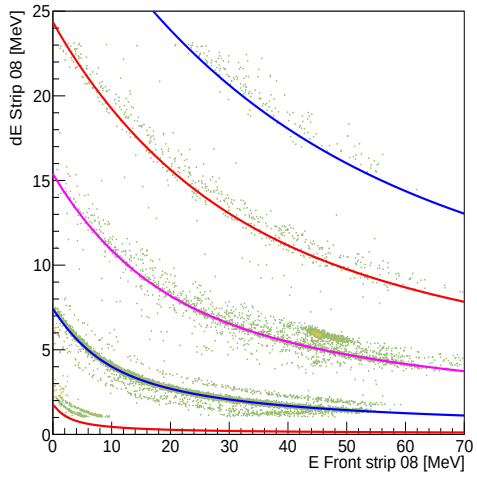

(b) An example of the fitted enhanced (14 parameters) LeNeindre function; for clarity, only one isotope per element is fitted.

Figure 3: dE-E histogram: (a) an example for one telescope data and (b) an example with fitted functional.

nucleus. Since a more detailed analysis is necessary to distinguish higher excited states from the background, only a few excited states above the desired decay threshold can be observed here.

3.2 α - α coincidences

As a first check of excited states reconstruction using the invariant mass method, the spectrum of two alpha particles detected in coincidence was used; shown in Fig. 4. There are a few key points worth mentioning. The first feature is a well-pronounced peak with high statistics at 0 MeV, corresponding to the ground state of ^{8}Be. Right next to it, at the energy of around 0.5 MeV, a peak that doesn't correspond to any expected or known ^{8}Be state can be observed. Such peak was previously observed in the measurements of the similar reactions [27–29]. It most probably originates from the alpha decay of ^{9}Be*, produced by both various reactions and beta-decayed ^{9}Li beam. At the energy of around 3 MeV, a broad bump is observed, which corresponds to the first ^{8}Be excited state (3.04 MeV, 2^{+}). It is slightly shifted to lower energies probably due to the efficiency of the detection setup.

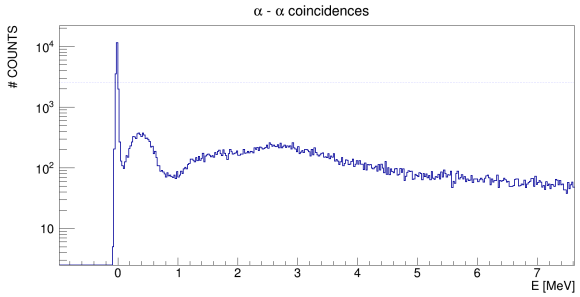

Figure 4: Invariant mass spectrum for two alpha particles detected in coincidence. The energy corresponds to the excitation energy of the assumed mother nucleus before decay.

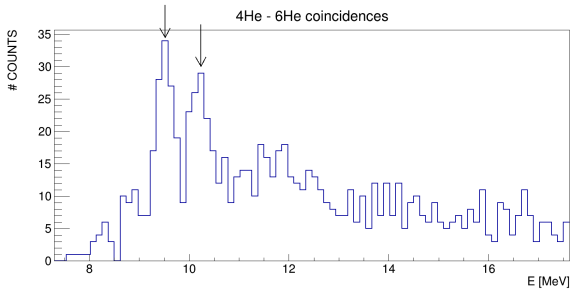

Figure 5: Invariant mass spectrum for α and ^{6}He detected in coincidence. Arrows show two peaks at the energies of around 9.5 MeV and 10.18 MeV. The energy corresponds to the excitation energy of the assumed mother nucleus before decay.

3.3 α - ^{6}He coincidences

The next interesting spectrum was reconstructed for ^{4}He and ^{6}He detected in coincidence, i.e. states which could correspond to the ^{10}Be excitations, shown in Fig. 5. The threshold for the alpha decay of ^{10}Be is at the energy of 7.4133 MeV, so observable peaks are expected above it. The very first state above the threshold, at the energy of 7.54 MeV, decays both via alpha decay and neutron emission. Therefore, alpha decay is suppressed due to the Coulomb barrier. The first alpha-decaying state we can observe (marked with the left arrow in Fig. 5) is peaked

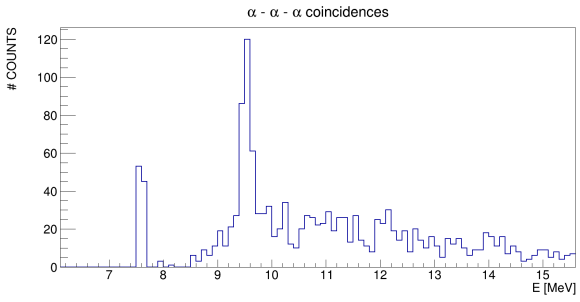

Figure 6: Invariant mass spectrum for three αs detected in coincidence. The energy corresponds to the excitation energy of the assumed mother nucleus before decay.

around 9.5 MeV. Right next to it is a state around 10.18 MeV (marked with the right arrow in Fig. 5). Even though, both peaks correspond to already studied states [7, 8, 30], the second one is still interesting and calls for further investigation. It is established as the 4^+ member of a rotational band built on the 0^+ state at 6.18 MeV [7, 29, 31]. Nevertheless, that state is still not fully characterized and it would be interesting to determine the partial widths of its known decay channels into ^{4}He + ^{6}He and ^{4}He + ^{6}He*. With additional statistics, this experiment might reveal higher excited states that correspond to the same rotational band.

In this spectrum, higher states are not well-pronounced, due to many possible reactions leaving ^{4}He and ^{6}He in the exit channel, which don't necessarily proceed through the excited states of ^{10}Be nucleus. Nevertheless, further data analysis will clear the spectra.

3.4 α - α - α coincidences

The final spectrum worth mentioning is the triple-alpha coincidence spectrum, i.e. excited states in ^{12}C. The threshold for the alpha-decay of ^{12}C is at 7.367 MeV, so again we are interested in states above it. In Fig. 6, two highly pronounced peaks can be observed. The first state is around 7.6 MeV while the other is around 9.6 MeV. They correspond to the Hoyle (0^+_2) and the 3^- state in ^{12}C nucleus, respectively.

4 Conclusion

In this contribution, preliminary results of the first part of the ^{9}Li on ^{11}B experiment performed at TRIUMF accelerator center are presented. This preliminary analysis aimed to determine the capability of correctly reconstructing fragments in coincidence and probing the excited states of a nucleus from which the fragments are emitted. The results presented here clearly show that some of the already well-known and highly clustered states in beryllium isotopes and ^{12}C are populated. That was expected as the experiment result since beryllium and carbon isotopes are populated through transfer reactions with high cross-section. These results prove the concept of the chosen beam and target to populate many different light nuclei with pronounced clustering or molecular structures. Furthermore, the presented results justify the selected detector setup as well-chosen for the desired state detection. In addition to the spectra presented here, many different coincidences were found, but there was insufficient statistical significance to be presented here. Pending the analysis of the second experimental campaign ran in August 2024, the presented results show the effectiveness of the chosen setup and open up new possibilities in further investigation of ^{10}Be rotational bands. With more detailed analysis and higher statistics gained, states of interest will be populated and studied using the chosen experimental setup.

Acknowledgements

We are grateful to Argonne National Laboratory's Target Fabrication Facility, target laboratory of INFN - LNL, and IFIN - HH target laboratory for providing the targets. The authors are also grateful for the high-quality beam delivered by the accelerators' operation staff at TRIUMF. This work was supported in part by the Croatian Science Foundation under project number HRZZ-MOBDOK-2023-1595 and Project no. IP-2018-01-1257 and by the U.S. Department of Energy, Office of Nuclear Physics, under Award No. DE-AC02-06CH11357.

References

[1] I. Lombardo, D. Dell'Aquila, Clusters in light nuclei: history and recent developments, La Rivista del Nuovo Cimento **46**, 521 (2023).

[2] M. Freer, Clustering in Light Nuclei; from the Stable to the Exotic (Springer Berlin Heidelberg, Berlin, Heidelberg, 2014), pp. 1–37, ISBN 978-3-642-45141-6, https://doi.org/10.1007/978-3-642-45141-6_1

[3] J.P. Ebran, E. Khan, T. Nikšić, D. Vretenar, How atomic nuclei cluster, Nature **487**, 341 (2012).

[4] L.R. Hafstad, E. Teller, The alpha-particle model of the nucleus, Phys. Rev. **54**, 681 (1938). 10.1103/PhysRev.54.681

[5] A.C. Shotter, A.N. Bice, J.M. Wouters, W.D. Rae, J. Cerny, Observation of the direct and sequential breakup of ^{7}Li from ^{12}C and ^{208}Pb targets at 70 mev, Phys. Rev. Lett. **46**, 12 (1981). 10.1103/PhysRevLett.46.12

[6] W. von Oertzen, M. Freer, Y. Kanada-En'yo, Nuclear clusters and nuclear molecules, Physics Reports **432**, 43 (2006). https://doi.org/10.1016/j.physrep.2006.07.001

[7] N. Soić, S. Blagus, M. Bogovac, S. Fazinić, M. Lattuada, M. Milin, D. Miljanić, D. Rendić, C. Spitaleri, T. Tadić, M. Zadro, ^{6}He + α clustering in ^{10}Be, Europhysics Letters **34**, 7 (1996). 10.1209/epl/i1996-00407-y

[8] M. Milin, M. Aliotta, S. Cherubini, T. Davinson, A.D. Pietro, P. Figuera, W. Galster, D. Miljanić,

A. Ninane, A.N. Ostrowski, A.C. Shotter et al., The ^{6}He + ^{6}Li reactions and exotic states of ^{10}Be, Europhysics Letters **48**, 616 (1999). 10.1209/epl/i1999-00528-3

[9] N. Vukman, N. Soić, M. Freer, M. Alcorta, D. Connolly, P. Čolović, T. Davinson, A. Di Pietro, A. Lennarz, A. Psaltis, C. Ruiz et al., Cluster decays of ^{12}Be excited states, Frontiers in Physics **10** (2022).

[10] Dell'Aquila, Daniele, Experimental studies of clustering in light nuclei: ^{11,12,13,16}C, Eur. Phys. J. Plus **135**, 165 (2020). 10.1140/epjp/s13360-020-00155-8

[11] D. Jelavić Malenica, M. Milin, S. Blagus, A. Di Pietro, P. Figuera, M. Lattuada, D. Miljanić, A. Musumarra, M.G. Pellegriti, L. Prepolec, V. Scuderi et al., ^{12}C states populated in ^{10}B+^{10}B reactions, Phys. Rev. C **99**, 064318 (2019). 10.1103/PhysRevC.99.064318

[12] D. Jelavić Malenica, M. Milin, D. Dell'Aquila, A. Di Pietro, P. Figuera, I. Gašparić, T. Mijatović, A. Musumarra, M.G. Pellegriti, V. Scuderi, N. Soić et al., The ^{13}C states populated in ^{10}B + ^{10}B reactions at 72 MeV, Eur. Phys. J. A **59**, 228 (2023).

[13] D.D. Zhang, Z.X. Ren, P.W. Zhao, D. Vretenar, T. Nikšić, J. Meng, Effects of rotation and valence nucleons in molecular α-chain nuclei, Phys. Rev. C **105**, 024322 (2022). 10.1103/PhysRevC.105.024322

[14] N. Itagaki, S. Okabe, K. Ikeda, I. Tanihata, Molecular-orbital structure in neutron-rich C isotopes, Phys. Rev. C **64**, 014301 (2001). 10.1103/PhysRevC.64.014301

[15] T. Baba, Y. Chiba, M. Kimura, 3α clustering in excited states of ^{16}C, Phys. Rev. C **90**, 064319 (2014). 10.1103/PhysRevC.90.064319

[16] Y. Liu, Y.L. Ye, J.L. Lou, X.F. Yang, T. Baba, M. Kimura, B. Yang, Z.H. Li, Q.T. Li, J.Y. Xu, Y.C. Ge et al., Positive-parity linear-chain molecular band in ^{16}C, Phys. Rev. Lett. **124**, 192501 (2020). 10.1103/PhysRevLett.124.192501

[17] J.X. Han, Y. Liu, Y.L. Ye, J.L. Lou, X.F. Yang, T. Baba, M. Kimura, B. Yang, Z.H. Li, Q.T. Li, J.Y. Xu et al., Observation of the $\pi^2\sigma^2$-bond linear-chain molecular structure in ^{16}C, Phys. Rev. C **105**, 044302 (2022). 10.1103/PhysRevC.105.044302

[18] TRIUMF, Isac facilities for rare-isotope beams (2024), last accessed 19 September 2024, https://www.triumf.ca/research-program/research-facilities/isac-facilities

[19] W.H. Ma, D. Patel, Y.Y. Yang, J.S. Wang, Y. Kanada-En'yo, R.F. Chen, J. Lubian, Y.L. Ye, Z.H. Yang, Z.Z. Ren, S. Mukherjee et al., Observation of ^{6}He + t cluster states in ^{9}Li, Phys. Rev. C **103**, L061302 (2021). 10.1103/PhysRevC.103.L061302

[20] F. Kobayashi, Y. Kanada-En'yo, Dinucleon correlations in the ground states of ^{9}Li, ^{10}Be, and ^{9,10}C, Phys. Rev. C **89**, 024315 (2014). 10.1103/PhysRevC.89.024315

[21] TUNL Nuclear Data Evaluation Project, Energy level diagram, ^{11}B (2012), https://nucldata.tunl.duke.edu/nucldata/figures/11figs/11_04_2012.png

[22] B. Harmatz, J. Shepard, Nuclear data sheets for A = 148, Nuclear Data Sheets **20**, 373 (1977). https://doi.org/10.1016/S0090-3752(77)80012-4

[23] Y. Ellis-Akovali, Nuclear data sheets of A = 230, Nuclear Data Sheets **40**, 385 (1983). https://doi.org/10.1016/S0090-3752(83)80076-3

[24] C. Nesaraja, Nuclear data sheets for A = 244, Nuclear Data Sheets **146**, 387 (2017). https://doi.org/10.1016/j.nds.2017.11.002

[25] L. Tassan-Got, A new functional for charge and mass identification in δe–e telescopes, Nucl. Instrum. Methods Phys. Res. B **194**, 503 (2002). https://doi.org/10.1016/S0168-583X(02)00957-6

[26] N. Le Neindre, M. Alderighi, A. Anzalone, R. Barnà, M. Bartolucci, I. Berceanu, B. Borderie, R. Bougault, M. Bruno, G. Cardella et al., Mass and charge identification of fragments detected with the *Chimera Silicon*-CsI(Tl) telescopes, Nucl. Instrum. Methods Phys. Res. A. **490**, 251 (2002).

[27] E.H. Berkowitz, G.L. Marolt, A.A. Rollefson, C.P. Browne, Survey of the ^{8}Be ghost anomaly, Phys. Rev. C **4**, 1564 (1971). 10.1103/PhysRevC.4.1564

[28] M. Madurga, M. Borge, H. Fynbo, B. Jonson, G. Nyman, Y. Prezado, K. Riisager, O. Tengblad, TONERRE collaboration, IS-417 collaboration, Multiple particle break-up study of low excited states in ^{9}Be: The ghost peak in the ^{8}Be excitation energy spectrum visited, Eur. Phys. J. Spec. Top. **150**, 137–138 (2007).

[29] M. Milin, M. Zadro, S. Cherubini, T. Davinson, A. Di Pietro, P. Figuera, D. Miljanić, A. Musumarra, A. Ninane, A. Ostrowski, M. Pellegriti et al., Sequential decay reactions induced by a 18 MeV ^{6}He beam on ^{6}Li and ^{7}Li, Nuclear Physics A **753**, 263 (2005). https://doi.org/10.1016/j.nuclphysa.2005.02.154

[30] TUNL Nuclear Data Evaluation Project, Energy level diagrams ^{10}Be (2004), last accessed 19 September 2024, https://nucldata.tunl.duke.edu/nucldata/figures/10figs/10_04_2004.gif

[31] M. Freer, E. Casarejos, L. Achouri, C. Angulo, N.I. Ashwood, N. Curtis, P. Demaret, C. Harlin, B. Laurent, M. Milin, N.A. Orr et al., $\alpha : 2n : \alpha$ molecular band in ^{10}Be, Phys. Rev. Lett. **96**, 042501 (2006). 10.1103/PhysRevLett.96.042501